International Conference on Space Optics—ICSO 2018

Chania, Greece

9–12 October 2018

Edited by Zoran Sodnik, Nikos Karafolas, and Bruno Cugny

Temperature control of a PM ring fiber cavity for long-term laser frequency stabilization

D. -H. Phung

J. -P. Coulon

M. Lintz

T. Lévèque

esa icso proceedings cnes

International Conference on Space Optics — ICSO 2018, edited by Zoran Sodnik, Nikos Karafolas, Bruno Cugny, Proc. of SPIE Vol. 11180, 1118054 · © 2018 ESA and CNES · CCC code: 0277-786X/18/$18 · doi: 10.1117/12.2536103

Temperature control of a PM ring fiber cavity for long-term laser frequency stabilization

D-H. Phung*[a], J-P. Coulon[a], M. Lintz[a], T. Lévèque[b]
[a]ARTEMIS, Université Côte d'Azur, Observatoire de la Côte d'Azur, CNRS, Nice, France
[b]CNES, 18 avenue Edouard Belin, 31400 Toulouse, France

ABSTRACT

We present a high performance, low cost, simple setup for long term temperature stabilization of a 2 m optical fiber ring cavity for laser frequency stabilization applications thanks to birefringence of the fiber and its dependence on temperature. The fiber temperature is controlled, at millisecond time scale by LED (light emissive diode) illumination. This allows reaching a temperature stability of 0.1 µK at 100 seconds for the 2 m long PM ring fiber cavity. This is a reduction of the fiber temperature by a factor of 2×10^5 (from 20 mK to 0.1 µK) and 5×10^5 (from 300 mK to 0.6 µK), at 100 seconds and at 10^5 seconds, respectively, with respect to the ambient temperature variations.

Keywords: Fiber ring cavity, Temperature stabilization, laser frequency stabilization, optical fiber birefringence

1. INTRODUCTION

Ultrastable lasers are typically realized by electronically locking the laser frequency to a resonance of an external reference cavity like Fabry-Perot cavity or whispering-gallery-mode resonators…When locking a laser to a fiber cavity, temperature drifts of the fiber are known to degrade the locked laser optical frequency on the long term due to the thermo-optic coefficient of silica, about 10^{-5} /K. In a different context, a dual-mode temperature measurement and stabilization has been implemented recently on two orthogonally polarized Whispering Gallery Mode (WGMs) [1, 2]. The shift of this “dual-mode beatnote frequency” can serve as a sensitive thermometer, and can be used as an error signal to control the 2 mm radius WGM resonator temperature by heating it with a light emitting diode (LED) [3]. In another experiment [4] an external heating laser was used for thermal control of an optical fiber Fabry–Perot resonator (FPF) to achieve a very high-speed tuning, at microsecond time scale, on cavity resonance frequency [4].

In this paper, we describe a high performance, low cost, simple setup for long term stabilization of a laser, where the role of the temperature sensor and of the optical reference cavity are played by the very same polarization maintaining (PM) fiber cavity. Two lasers can be frequency locked on the modes corresponding to two orthogonal polarization axes of a PM fiber ring cavity. The latter is obtained (realized from a commercial, low loss, low ratio tap coupler, by connecting two of the four ports). The laser polarization is made to match the slow axis polarization, and the fast axis polarization, respectively. Then, thanks to birefringence of the fiber and its dependence on temperature, the two lasers’ beat-note frequency turns out to be an efficient temperature discriminator, and can be used in a loop that controls the fiber temperature. The cavity temperature is controlled, at millisecond time scales by LED illumination of the fiber. This allows reaching a temperature stability of 0.1 µK at 100 seconds for the 2 m long PM ring fiber cavity. The noise-budget analysis shows that thermal drifts of several offsets in electronic circuits mainly limits the long-term stability, and need to be dealt with at the required level.

2. DOUBLE LASER LOCKING – THEORETICAL PRINCIPE

2.1 Polarization Maintaining Fiber Ring Cavity

The fiber ring cavity, obtained by fusion splicing the two tap ports of a low-ratio PM coupler, can be described by the optical transmission T and reflection $R \ll T$ of the coupler, Figure 1

***duy-ha.phung@oca.eu; phone +33 (0)4 92 00 31 98; artemis.oca.eu/fr/accueil-artemis**

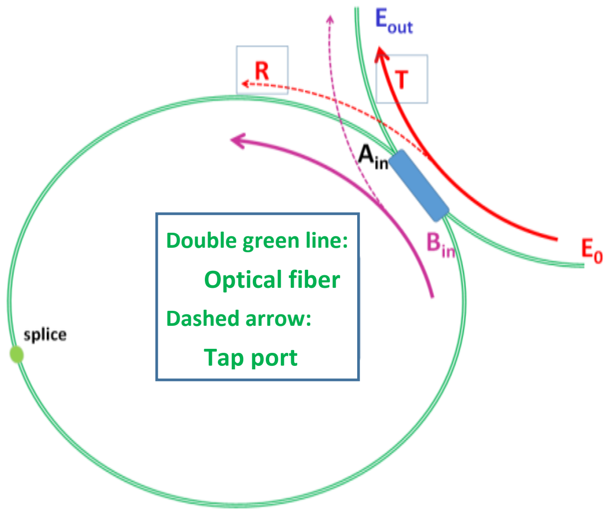

Figure 1. The fiber ring cavity - obtained by fusion splicing the two tap ports of a low-ratio PM coupler

The transfer function of the cavity between output E_{out} and input optical wave $E_0 = e^{i\omega t}$, is given by:

$$\frac{E_{out}}{E_0} = \frac{\sqrt{T} - (T+R)e^{i\varphi}}{1 - \sqrt{T}e^{i\varphi}} \tag{1}$$

Where $\varphi = 2\pi v n L/c = \omega n L/c$ is the delay phase caused by the fiber ring length, v is the optical frequency of the laser source, n the fiber refraction index, L the fiber length of ring cavity, c the light velocity in vacuum.

The ideal case without loss, $T + R = 1$, was applied in this analysis. See Sect. 2.2 for the case of non-zero losses. As the index n is slightly different for the two polarizations of the PM fiber, the free spectral range (FSR) c/nL is slightly different and the two combs of modes are shifted from each other.

The phase of the transfer function is written as:

$$\phi = atan\left[\frac{(T-1)sin(\varphi)}{2\sqrt{T} - (T+1)cos(\varphi)}\right] \tag{2}$$

The cavity finesse, Γ, determined by the ratio between a 2π cycle and the $\Delta\varphi = \varphi(\phi = \pi/2) - \varphi(\phi = -\pi/2)$ phase separation, may be approximated by $\Gamma \approx 6/R$. Finesse is about 59.6 when R = 10%, 122 when R = 5% and 292 when R = 2%.

2.2 Real case with loss in fiber ring cavity

The loss in the ring cavity (Figure 1) may be modelled by coupler insertion loss, L_c and ring fiber loss L_i. The reflection and transmission ratios R, T, can be redefined using the R_0 and $T_0 = (1 - R_0)$ ideal ratios.

$$R = (1 - L_c)R_0; \quad T = (1 - L_c)(1 - R_0) \tag{3}$$

The ideal transfer function; eq. 1, becomes:

$$\frac{E_{out}}{E_0} = \frac{\sqrt{T} - (1 - L_c)\sqrt{(1 - L_i)}e^{i\varphi}}{1 - \sqrt{T(1 - L_i)}e^{i\varphi}} \equiv K(\omega) \tag{4}$$

In this case, the cavity finesse depends also on coupler loss and ring cavity fiber loss, and can be written as:

$$\Gamma \approx \frac{\pi\sqrt[4]{(1 - L_c)(1 - L_i)(1 - R_0)}}{1 - \sqrt{(1 - L_c)(1 - L_i)(1 - R_0)}} \tag{5}$$

When the coupler loss is 10%, it can reduce the finesse from 59.6 ($R_0 = 10\%$), 122 ($R_0 = 5\%$), and 292 ($R_0 = 2\%$) to 29.9, 40.3 and 50.4, respectively.

The Figure 2 below shows the transmission spectra recorded with fiber ring cavities made with ComCore [5] and OzOptics [6], fiber couplers. The finesses measured in slow axis and fast axis are shown in the table I.

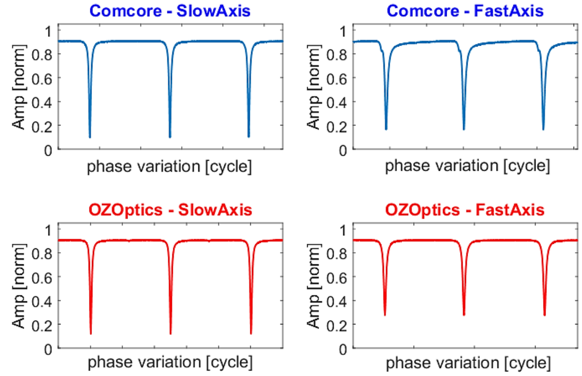

Figure 2. Measured transmission through the resonators obtained from ComCore and OzOptics couplers.

Table 1. Finesse and contrast measured with ComCore and OzOptics PM couplers in slow and fast axis.

	ComCore		**OzOptics**	
	Slow Axis	Fast Axis	Slow Axis	Fast Axis
Finesse	38	36	41	29
Contrast	0.80	0.69	0.76	0.53

2.3 Locking on cavity – Pound-Drever-Hall setup

The error signal is formed with a Pound-Drever-Hall setup [7]. A phase modulation is imprinted onto the laser beam before the cavity input. The modulation signal is characterized by its amplitude β and frequency δ, with $\Omega = 2\pi\delta$. For small angle expansion, we can consider that:

$$E_0 = e^{i[\omega t + \beta sin(\Omega t)]} \approx \left(1 + \frac{\beta}{2} e^{i\Omega t} - \frac{\beta}{2} e^{-i\Omega t}\right) e^{i\omega t} \tag{6}$$

so that we have a carrier and two sidebands, and the beam E_{out} at the output of the resonator is:

$$E_{\text{out}} = K(\omega) e^{i\omega t} + \frac{\beta}{2} K(\omega + \Omega) e^{i(\omega+\Omega)t} - \frac{\beta}{2} K(\omega - \Omega) e^{i(\omega-\Omega)t} \tag{7}$$

Where K is defined in eq. 4, $K(\omega) = K_0(\omega) e^{i\phi(\omega)}$ as a function of $\omega = 2\pi\nu$.

The power of the output beam, measured by a photodetector, is given by:

$$\begin{aligned} P_{\text{out}} = {} & |K(\omega)|^2 + \tfrac{1}{4}\beta^2[|K(\omega+\Omega)|^2 + |K(\omega-\Omega)|^2] \\ & + \beta Re[K(\omega)K^*(\omega+\Omega) - K(\omega)K^*(\omega-\Omega)]\cos(\Omega t) \\ & + \beta Im[K(\omega)K^*(\omega+\Omega) - K(\omega)K^*(\omega-\Omega)]\sin(\Omega t) \\ & + 2\Omega \text{ terms} \end{aligned} \tag{8}$$

A mixer converts the term that is proportional to $\sin(\Omega t)$ into an error signal:

$$\varepsilon(\omega) = \beta\, Im[K(\omega)K^*(\omega+\Omega) - K^*(\omega)K(\omega-\Omega)] \tag{9}$$

Figure 3 below shows the error signal shape at amplitude modulation $\beta = 0.5$ and for several values of the frequency of modulation $\delta = \Omega/2\pi$. The calculation is performed for 2 m fiber ring cavity, $FSR \approx 100$ MHz (1 cycle), without loss $R = 0.1,\ \text{T} = 0.9$ In Figure 3 below, one horizontal division equals to about of 10 MHz.

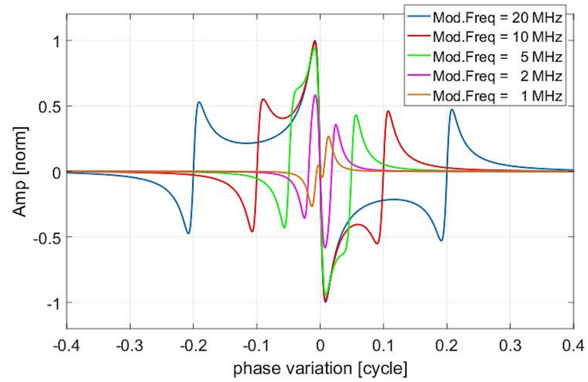

Figure 3. Error signal shape for the ideal case, FSR = 100 MHz, R = 0.1

For a 2 m fiber ring cavity, the modulation frequency should be selected between 5 and 20 MHz to have an error signal with appropriate size and shape for the PDH locking.

2.4 Double lock theory with a birefringent fiber ring cavity

The cavity is characterized by the fiber length L, indices $n_\perp$ and $n_\parallel$ corresponding to the two polarizations. Corresponding free spectral range FSR are defined by $FSR_\perp = c/n_\perp L$, $FSR_\parallel = c/n_\parallel L$. The two lasers are locked on two modes $\nu_\perp = N_\perp FSR_\perp$ and $\nu_\parallel = N_\parallel FSR_\parallel$ according to the two different polarizations where $N_\perp$ and $N_\parallel$ are constant integers. With a fiber ring length of 2 m, $N_\perp$ and $N_\parallel$ are about 1.94×10^6 for 1550 nm lasers. The beatnote frequency between the two lasers is given by:

$$F = \frac{c}{L}\left[\frac{N_\perp(n-\Delta n/2) - N_\parallel(n+\Delta n/2)}{n^2 - \Delta n^2/4}\right] \tag{10}$$

where $n \equiv (n_\perp + n_\parallel)/2$ is the average index, and $\Delta n \equiv (n_\perp - n_\parallel)$ is the birefringence of the fiber.

Birefringence in PM1550 fiber is about $\Delta n \approx 4.65 \times 10^{-4}$ [8]. Thus, Δn^2 can be neglected, the beatnote frequency is rewritten by:

$$F \approx \frac{c}{nL}\left[(N_\perp - N_\parallel) - \frac{\Delta n}{2n}(N_\perp + N_\parallel)\right] = \frac{c}{nL}\Delta N - \frac{\Delta n}{n}\nu \tag{11}$$

where $\Delta N \equiv N_\perp - N_\parallel, \nu \equiv c/nL \times (N_\perp + N_\parallel)/2$. Figure 4 below shows the contributions of the two terms in the beatnote frequency magnitude when $N_\perp - N_\parallel$ is scanned at given $N_\perp + N_\parallel$ for various cavity fiber lengths.

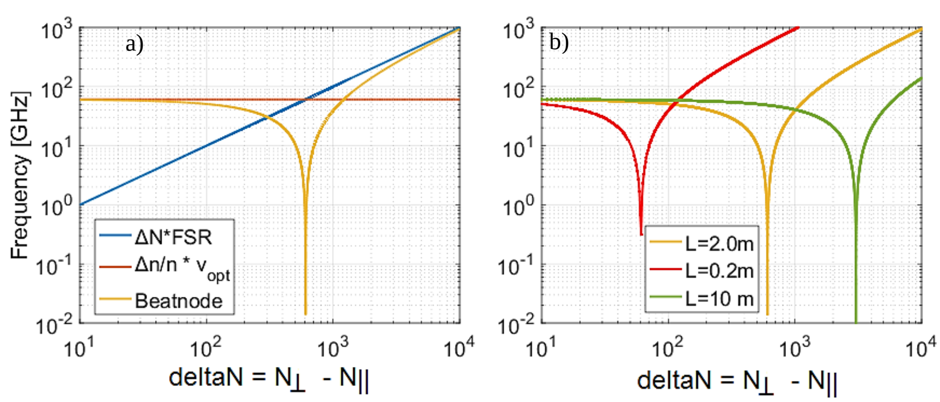

Figure 4. Beatnote frequency (absolute value) and contributions from the two terms of eq.11.
a) Contribution of from two terms of eq.11 for L = 2 m; b): beatnote frequency for 3 fiber lengths of 0.2 m, 2.0 m and 10 m

This estimation shows that, for a fiber length of 2 m, when ΔN is smaller than 100, beatnote frequency is dominated by $\Delta n/n \times \nu$ term, and close to 55 GHz. When ΔN is bigger than 1000, beatnote frequency increases linearly with ΔN. To correctly characterize beatnote frequency, the two lasers must be adjusted on frequency for achieving a beatnote frequency small enough to be reasonably convenient for PDH locking, say, from several tens MHz to several GHz corresponding to the zone [500, 700] of ΔN.

Let us now consider locked operation, that is, $N_\perp$ and $N_\parallel$ are fixed integers: in a temperature variation, the beatnote frequency varies because of isotropic index variation, $(n_\perp + n_\parallel)/2$ term, and because of differential sensitivity, $(n_\perp - n_\parallel)/2n$ term. The fractional sensitivity of the beatnote frequency to the temperature can be estimated by:

$$\left|\frac{dF}{FdT}\right| \approx \left|\frac{dL}{LdT} + \left(1 - \frac{\Delta n}{n}\frac{\nu}{F}\right)\frac{dn}{ndT} + \frac{\nu}{F}\frac{d\Delta n}{ndT}\right| \tag{12}$$

For a PM fiber (cladding-SiO2), thermal expansion coefficient dL/LdT is about of $5 \times 10^{-7}\ K^{-1}$, thermal coefficient for index dn/ndT is about of $6 \times 10^{-6}\ K^{-1}$ and the group birefringence thermal coefficient $d\Delta n/dT$ is about of $4.1 \times 10^{-7}\ K^{-1}$ [8]. With fiber length of 2 m, we expect a fractional beatnote thermal sensitivity dF/FdT of $0.054\ K^{-1}$ when the beatnote is about 1 GHz. In Figure 5-a, we note that thermal effect on PM fiber is dominated by birefringence thermal effect (differential effect on fiber index), the frequency shift is 300 times bigger than isotropic index effect. The contribution from fiber expansion is negligible.

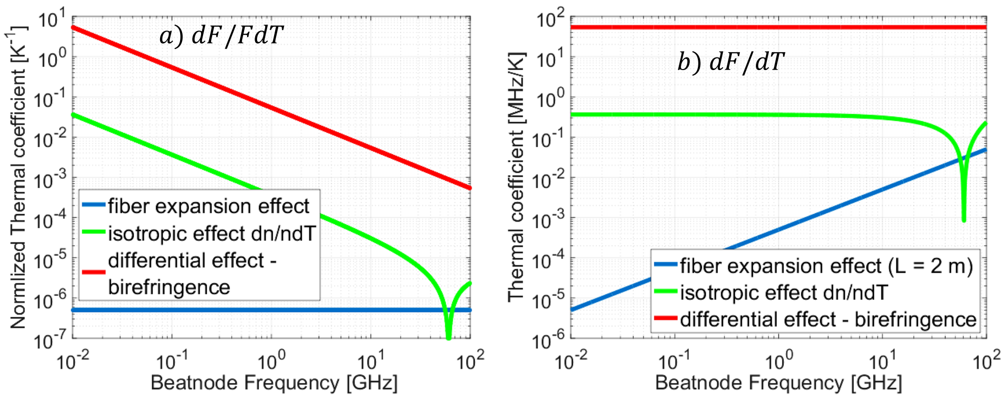

Figure 5. a) Fractional thermal deviation of beatnote frequency (dF/FdT) following beatnote frequency F
b) Thermal deviation of beatnote frequency (dF/dT) following beatnote frequency F

Figure 5-b shows that the thermal coefficient dF/dT is essentially independent of the beatnote frequency. Its value of about 50 MHz/K or 50 Hz/μK that can provide a highly sensitivity temperature discriminator from frequency measurement.

3. Experiment setup and results

3.1 Double laser lock to fiber ring cavity

Two 1542 nm sources, Koheras – E15 Adjustik lasers, are used in the experiment, with a spectral linewidth of 5 kHz (measured at 100 ms), their frequencies are tunable by temperature and high-speed piezo controllers. To generate the two PDH error signals, one laser is modulated in frequency at 10.1 MHz, the other one at 12.0 MHz by two fibered electro/optic phase-modulators (MPX-LN-0.1 from Photline). The two modulated lasers are combined by a polarized beam combiner/splitter and sent to the fiber cavity at the two orthogonal polarizations (slow and fast axis) of the PM fiber. The transmitted beam, containing resonance information for the two laser sources at the two polarizations, is detected by the same photodiode (Thorlabs DET10C/M). Two identical Pound Drever Hall locking systems, developed by the laboratory, demodulate the photodiode signal (at respectively 10.1 MHz and 12.0 MHz) and lock the two lasers on two modes of the cavity with 1.5 kHz bandwidth using the piezo laser frequency actuators. 10.1 MHz instead of 10.0 MHz is selected for one of the two channels to avoid cross-talks in the demodulated signal caused by high harmonics mixing that occurs when the two frequencies are exactly 12.0 MHz and 10.0 MHz. 10% of optical power from two lasers are dedicated to the two PDH locking systems, and 90% is dedicated to the user, out of which we use 10% of for beatnote detection by a fibered EM4 18 GHz photodiode.

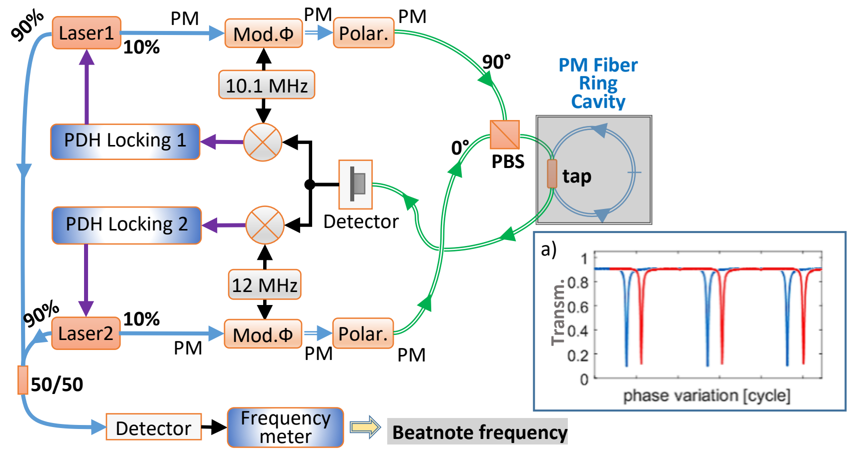

Figure 6. Double laser lock (Pound Drever Hall scheme) on a fiber ring cavity.
a) Two successive fiber ring cavity Transmission curves as a function of the laser frequency, measured with two orthogonal polarizations. Laser 1, 2: 1542 nm – fiber laser sources; PDH Locking: Pound Drever Hall servo electronics; tap: fiber tap coupler; Mod.Φ: LiNbO3 Phase modulator; Polar: Fibered polarization controller; Detector: InGaAs Photodiode; 50/50: beam splitter

Figure 7 shows first experiment result with double laser lock, beatnote frequency and cavity temperature were recorded during 6 hours, beatnote frequency is measured by a frequency-meter, Anritsu MF2414A. During this 0.4 °C ambient temperature variation, the beatnote frequency shows a dependence of about 44 MHz/K, and the frequencies of two lasers vary approximately at 1400 MHz/K from piezo correction signal of PDH locking system (Figure 7-b), these measured thermal coefficients are consistent with theoretical estimates.

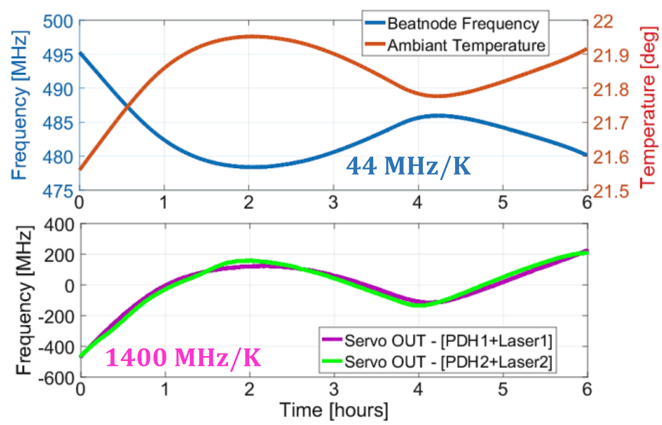

Figure 7. Experiment: simultaneous recording of the ambient temperature and beatnote frequency (upper graph), and of the correction signals of the two lasers, converted into optical frequency (lower graph).
Signal – thermal coefficients of beatnote frequency and laser frequency. The green curve (piezo correction signal of PDH2+Laser2) fluctuates more than that of PDH1+Laser1 because the Laser2 is more unstable than Laser1 when ambient condition change (temperature, humidity, pressure …)

This result shows that the beatnote frequency is a very high sensitivity discriminator of fiber ring temperature at sub-μK scale, and suggests us a simple, high performance setup for temperature stabilization of fiber ring cavity. In the next section, we discuss how to control fiber ring cavity temperature from beatnote frequency when the two lasers are locked on the cavity.

3.2 Ring cavity fiber temperature controller

In this section, we present how to mount the 2 m length ring fiber cavity to control its temperature. The main idea is that temperature of the ring cavity is regulated by a Peltier unit at long time range and by LED illumination at short time range – as discussed in section III-C. For this configuration, we need to put the fiber ring cavity in a thermally insulated, thick aluminium enclosure of ∅ = 200 mm in Figure 8, for preliminary stabilization of its temperature. The aluminium enclosure is placed on 4 Peltier units contacted (by thermal paste) to an aluminium plate (300 x 600 mm) heated by 3 heating mats (in orange, below the plate, Figure 8) to allow us to set quickly the approximate temperature for the aluminium enclosure. The ring cavity and temperature sensors (four10kΩ thermistors in series distributed around the ring cavity) are placed together between two spherical metal reflectors (∅ = 120 mm, Figure 9). 3 white LEDs are fixed on each reflector to create a two-sided illumination for the ring cavity.

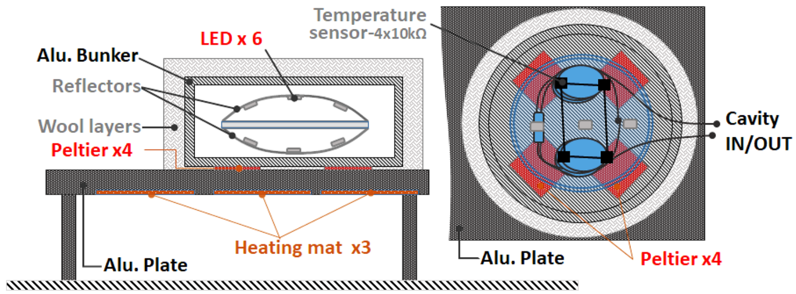

Figure 8. Fiber ring cavity mounted in the ∅= 200 mm thermal enclosure

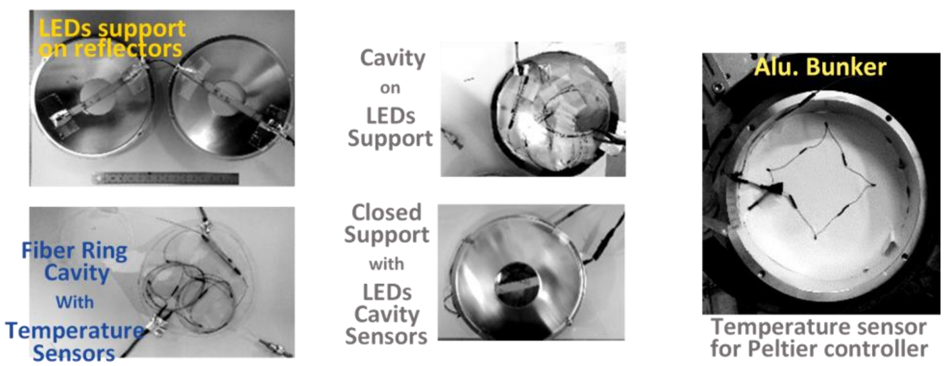

Figure 9. Mounting fiber ring cavity and six LEDs between two reflectors

The Figure 10 below shows the block diagram of cavity temperature control. To stabilize ring cavity temperature at long time range, 4 Peltier unit are controlled firstly by observing enclosure temperature (detected from thermistors lying at the enclosure bottom), and maintain it around T_0 = 35 degrees when ambient temperature varies between 24 – 27 °C in our experiment. LED current is controlled directly to stabilize the beatnote frequency using LED light absorption in the fiber coating, painted beforehand with usual black ink for efficient control. The response of the beatnote frequency under LED illumination is discussed in section III-C.

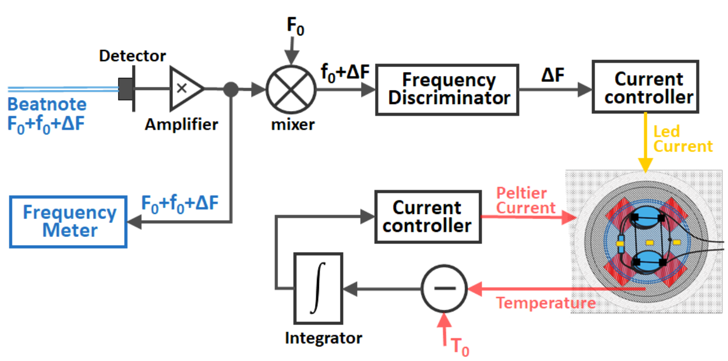

Figure 10. Block drawing of the ring cavity temperature control system with two channels for beatnote frequency measurement

The beatnote detected by EM4 photodiode is amplified and divided in two channels, one for slow, high resolution frequency measurement (F0+f0+ΔF, by frequency-meter at one measure per 2.5 seconds). The other one is dedicated for high-speed frequency measurement (ΔF, by a frequency discriminator providing Hz-to-voltage conversion) to track quickly beatnote frequency variations and send corrections to LED current controller in order to stabilize beatnote frequency and fiber ring cavity temperature.

The division in short and long time range accounts for the fact that LED illumination is powerful enough to give rise to a 1K resonator temperature rise, because the thermal mass of the fiber is very small, but not powerful enough to give rise to the same temperature rise of the aluminum enclosure (about 2 kg) to compensate large variation of ambient temperature (about several degrees). The locking system with 4 Peltier unit, mounted as in Figure 9, can maintain the enclosure temperature with a deviation of several mK when ambient temperature varies several degrees, shown in Figure 11.

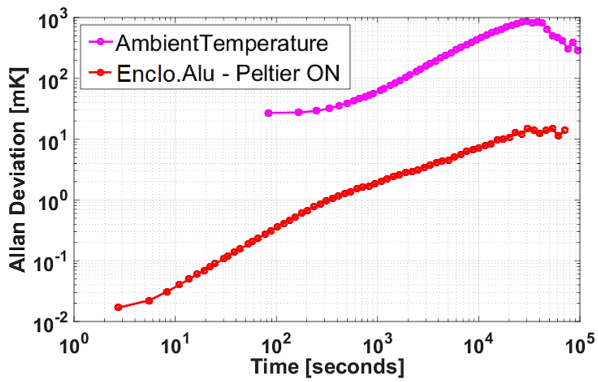

Figure 11. Allan deviation of ambient temperature and enclosure temperature when Peltier locking is activated

In this condition - one or a few tens of mK stability, the LED current controller is able to compensate and stabilize the ring cavity temperature to <µK, presented in the section III-C following. From now, one defines that ring cavity temperature variation is the temperature variation calculated from the measured beatnote frequency with thermal coefficient of 44 MHz/K, and enclosure temperature is the directly measured temperature by thermistor sensors in the enclosure.

Because of large thermal mass, the whole system (aluminum enclosure, plate) takes several minutes to reach a steady temperature. In addition, at very long time range (1 day), the fiber resonator temperature can change under large ambient temperature variations because the controller loop gain is not high enough at this very long time range. To solve this issue, we try to integrate beatnote frequency variation at very long time range, and use this integrated signal to change the setting temperature of the insulated enclosure in order to offload LED illumination system and to achieve the stability of the beatnote frequency at this long time range. The Figure 12 shows the block diagram of addition channel for Peltier controller. This configuration allows us to improve by a factor of 3 or 4 the cavity ring temperature stability at very long time range (> 10^4 seconds). In the section III-C, we present also the result when addition channel is not activated.

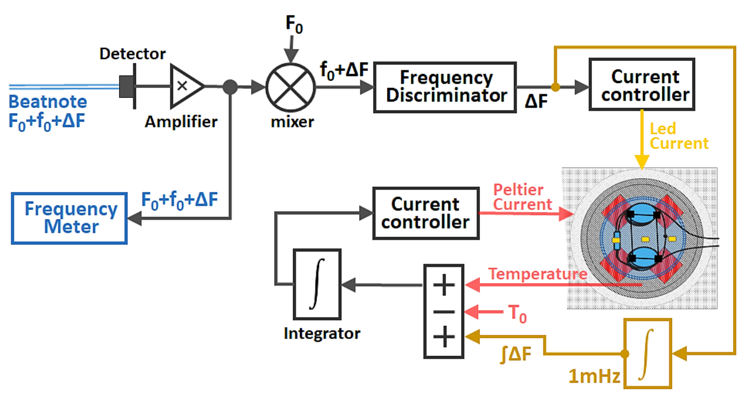

Figure 12. Block drawing of ring cavity temperature control system with 3 channels

In this way, when LED current controller is activated, both beatnote frequency and enclosure temperature are stabilized at both short and long term. Figure 13 shows raw data of beatnote frequency when we activate LED locking system, it gives us first idea of locking performance. These results are detailed and discussed in the following sections.

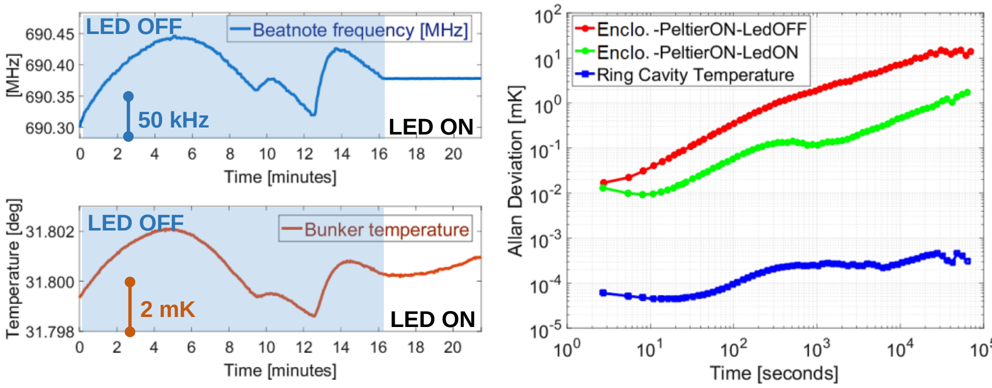

Figure 13. Beatnote frequency raw data and Allan deviation (converted to temperature) before and after activation of LED locking system

3.3 Transfer function of Beatnote frequency versus LED current

The ring cavity temperature (2 m fiber) varies when the fiber absorbs LED light. By modulating LED current (12 V, 20 mA in total, equivalent to 0.25 W variation), cavity temperature can be varied 0.35 mK at 10 Hz (or 100 ms), Figure 14-a. That is equivalent to a variation of 500 kHz on laser optical frequency and 16 kHz on beatnote frequency. In addition, we notice that the reaction time of ring cavity temperature is sub-ms when we turn on/off the LEDs, Figure 14-b, c, deduced from PDH piezo correction and beatnote frequency variations.

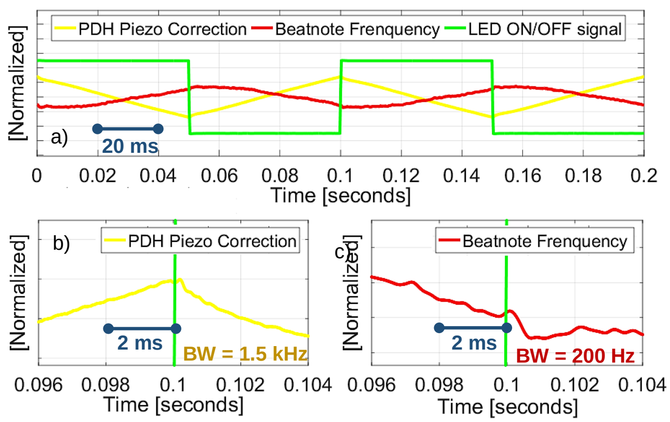

Figure 14. Beatnote and optical laser frequency variation when turning LEDs on/off at 10 Hz
a) Yellow curve: PDH Piezo correction – optical laser frequency, Isotropic effect ≈ 500 kHz amplitude; Red curve: beatnote frequency, birefringence effect ≈ 15 kHz amplitude ($\Delta T \approx 0.34$ mK at 3.4μK/ms); Green curve: LED on/off signal
b) Zoom on 8 ms of PDH Piezo correction; c) Zoom on 8ms of Beatnote frequency variation.

The different behaviour between beatnote frequency variation and PDH Piezo correction at millisecond scale when the LED was turned on (after 0.1 s moment in Figure 14-b, -c) can be explained by 200 Hz bandwidth at of our frequency discriminator (analog frequency discriminator, using the commercial POS+75 VCO from Minicircuits).

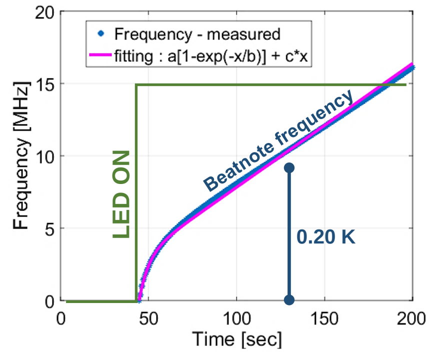

Figure 15. Temporal response at long time range of ring cavity temperature

At long time range, several seconds, LED illumination can change ring cavity temperature of 0.35 degree after 150 seconds, blue curve in Figure 15. The variation of beatnote frequency can be fitted by a sum of two terms – an exponential with a time constant of 5.1 s and linear term or more exactly, it is an exponential term with a large time constant.

Figure 16 shows PDH Piezo correction and beatnote frequency modulations when we modulate LEDs current at various frequencies. These transfer functions confirm that thermal absorption effect of fiber ring cavity can be characterized like a clean integrator, $1/f$ on amplitude and 90 degrees on phase. It allow us to have a correct design for LED current locking system by beatnote frequency variation signal, shown in Figure 12.

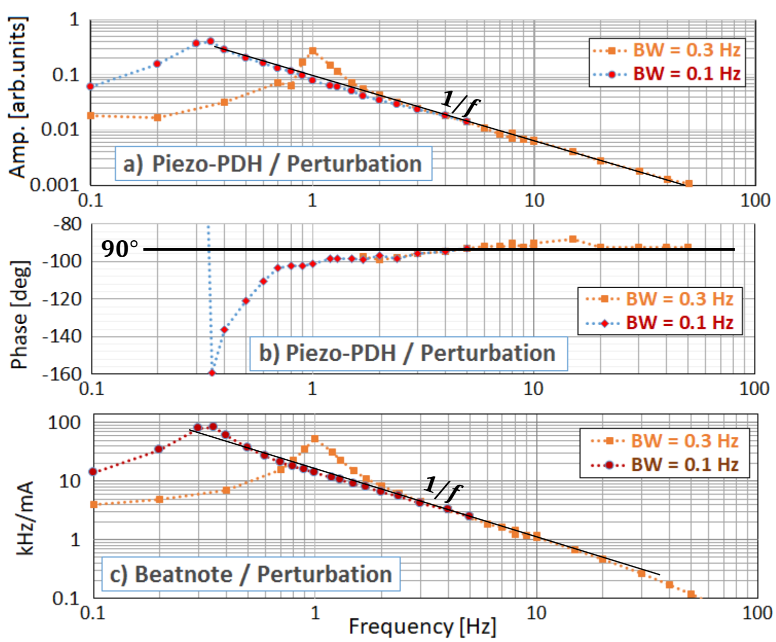

Figure 16. Transfer function shapes of PDH piezo correction & beatnote frequency versus LED current
a) Amplitude and b) Phase of transfer function between PDH piezo correction and LED current
c) Amplitude of transfer function between beatnote frequency and LED current
Enclosure temperature locking system was locked at 0.3 Hz and 0.1 Hz to prevent slow temperature drifts during this measurement, that explains 1 Hz (on orange dots-curve) and 0.3 Hz (on red dots-curve) peaks. The transfer functions are obtained by dividing the system response by the applied perturbation.

Converted to ring cavity temperature versus LED current, transfer function can be modelled by $0.2/f$ [mK/mA]. This parameter will be used as input to select an appropriate gain for the temperature locking system design. In the next section, we show some experimental results of ring cavity temperature when current LED locking is active.

3.4 Cavity temperature stability with LED illumination controller

Figure 17 shows Allan deviation corresponding to different temperatures to characterize their stability as functions of time when LED current controller is activated. While temperature varies daily of 2.5 degrees, the temperature controllers (Peltier and LED) can maintain the enclosure temperature at < 10 mK and cavity ring temperature at 10^{-7} K.

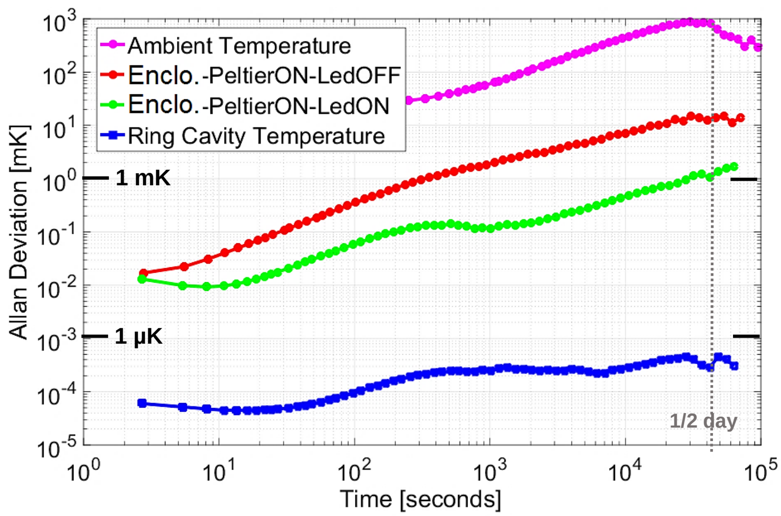

Figure 17. Allan deviation of ambient temperature, enclosure temperature and ring cavity temperature
Magenta curve: deviation of ambient temperature; red curve: deviation of enclosure temperature when LED current controller was off; green curve: deviation of enclosure temperature when LED current controller was active; blue curve: deviation of ring cavity temperature, obtained from beatnote frequency measurement. Enclo: aluminum enclosure.

We achieve an attenuation factor of 500 between enclosure temperature and cavity ring temperature when LED current controller is activated.

This result confirms that the cavity temperature can be controlled and maintained to sub µK by the LED illumination method using beatnote frequency as the error signal for the LED current controller. This allows reaching a temperature stability of 0.1 µK up to 100 seconds for the 2 m long PM ring fiber cavity. As compared to the ambient temperature stability, this is an improvement by a factor of $2{\times}10^5$ (from 20 mK to 0.1 µK) and 10^6 (from 600 mK to 0.6 µK of fiber cavity temperature), at 100 seconds and at $10^4 – 10^5$ seconds, respectively.

Table 2. Stability improvement factor between ambient temperature and ring fiber cavity temperature

Time scale	100 seconds	$10^4 – 10^5$ seconds
Gain in temperature stability	100000	1 million

4. Conclusion

We have demonstrated a very simple, high performance setup, operating at room temperature for sub µK temperature stabilization off a 2m optical fiber ring cavity at long term (up to 100000 seconds), based on the thermal dependence of the fiber birefringence and LED illumination. Our set-up is based on commercially available components of the telecom industry. To the best of our knowledge, this is the first demonstration of sub µK temperature stabilization on a 2 m optical fiber. The present long term temperature stabilization of our approach is limited by thermal drifts of several offsets in electronic circuits (from PDH error signals, from offsets of Peltier controller circuit, from LED offset current, from lock loop Gain at very long time range,...). It also should be pointed out that in addition to the thermal dependence of the fiber birefringence, the measured beatnote frequency may have other dependencies, for example, on the humidity, or the atmospheric pressure around the fiber ring cavity). More investigations on these drifts and beatnote dependencies will be the subject of our future work.

Since the main object of our demonstrated optical fiber temperature stabilization setup is to provide a stable laser, it is interesting to estimate the projected fractional frequency stability of two laser sources locked to the fiber ring cavity. According to the figure 17, by using the factor of 30 between thermal sensitivities of laser frequencies and beatnote frequency, we expect to be able to stabilize our laser frequencies to 3.8×10^{-13} at 3 seconds, to 6×10^{-13} at 100 seconds, and to 3.1×10^{-12} per $10^3 - 10^5$ seconds. This expected result is promising when comparing to performance of 1.3×10^{-12} at 1.0 second and 1.1×10^{-10} at 1000 seconds [3] where the authors used the same technical (crystal birefringence thermal dependence [9] and LED illumination) on an MgF_2 single crystal WGM resonator with 1560 nm lasers sources.

ACKNOWLEDGEMENTS

The author acknowledges financial support from Labex FIRST-TF.

REFERENCE

[1] D. V. Strekalov, R. J. Thompson, L. M. Baumgartel, I. S. Grudinin, and N. Yu, "Temperature measurement and stabilization in a birefringent whispering gallery mode resonator," *Opt. Express* 19 (15), 14495–14501 (2011).
[2]. L. Baumgartel, R. Thompson, D. Strekalov, I. Grudinin, and N. Yu, "Dual Mode Frequency Stabilization of a Whispering Gallery Mode Optical Reference Cavity," in CLEO: Science and Innovations, *OSA Technical Digest* (online), CTh3A.6. (2012).
[3] I. Fescenko, J. Alnis, A. Schliesser, C. Y. Wang, T. J. Kippenberg, and T. W. Hänsch, "Dual-mode temperature compensation technique for laser stabilization to a crystalline whispering gallery mode resonator," *Opt. Express* 20, 19185-19193 (2012)
[4] J. Gallego, S. Ghosh, S.K. Alavi *et al*. "High-finesse fiber Fabry–Perot cavities: stabilization and mode matching analysis",*Appl. Phys. B* 122: 47, (2016).
[5] OZ-Optics, Polarization maintaining fused fiber couplers/splitter, `https://www.ozoptics.com/ALLNEW_PDF/DTS0092.pdf`
[6] Comcore Technologies Inc., 1x2(2x2) Fused PM Fiber Standard Splitter `http://www.comcore.com/PDF/product0004.pdf`
[7]. R.W.P. Drever; J.L. Hall; F.V. Kowalski; J. Hough; G.M. Ford; A.J. Munley; H. Ward, "Laser phase and frequency stabilization using an optical resonator", *Appl. Phys. B*.31(2): 97–105, (1983).
[8] Zhihong Li, X. Steve Yao, Xiaojun Chen, Hongxin Chen, Zhuo Meng, and Tiegen Liu, "Complete Characterization of Polarization-Maintaining Fibers Using Distributed Polarization Analysis," *J. Lightwave Technol*.33, 372-380 (2015)
[9] A. B. Matsko, A. A. Savchenkov, V. S. Ilchenko, D. Seidel, and L. Maleki, "Optical-RF frequency stability transformer," *Opt. Lett.* 36, 4527–4529 (2011).